JACS
JOURNAL OF THE AMERICAN CHEMICAL SOCIETY
Article
pubs.acs.org/JACS

Temperature-Independent Singlet Exciton Fission in Tetracene

Mark W. B. Wilson,*[,‡] Akshay Rao, Kerr Johnson, Simon Gélinas, Riccardo di Pietro,[¶] Jenny Clark, and Richard H. Friend*

Cavendish Laboratory, University of Cambridge, Cambridge CB3 0HE, U.K.

Supporting Information

ABSTRACT: We use transient absorption spectroscopy to demonstrate that the dynamics of singlet exciton fission in tetracene are independent of temperature (10−270 K). Low-intensity, broad-band measurements allow the identification of spectral features while minimizing bimolecular recombination. Hence, by directly observing both species, we find that the time constant for the conversion of singlets to triplet pairs is ∼90 ps. However, in contrast to pentacene, where fission is effectively unidirectional, we confirm that the emissive singlet in tetracene is readily regenerated from spin-correlated "geminate" triplets following fission, leading to equilibrium dynamics. Although free triplets are efficiently generated at room temperature, the interplay of superradiance and frustrated triplet diffusion contributes to a nearly 20-fold increase in the steady-state fluorescence as the sample is cooled. Together, these results require that singlets and triplet pairs in tetracene are effectively degenerate in energy, and begin to reconcile the temperature dependence of many macroscopic observables with a fission process which does not require thermal activation.

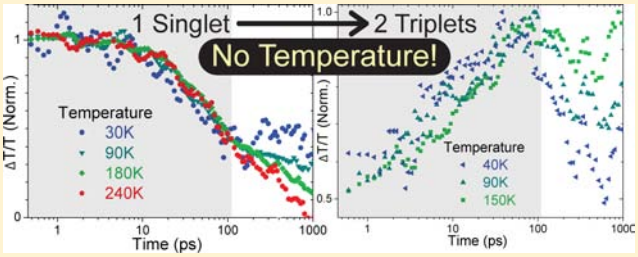

INTRODUCTION

Singlet exciton fission is the process in organic semiconductors by which a single photoexcited spin-singlet exciton generates two spin-triplet excitons on nearby chromophores.[1] Singlet fission is spin-allowed, differing from spin−orbit-mediated intersystem crossing as triplets are created in a singlet-coupled pair state. Although this carrier multiplication process was first studied more than four decades ago,[2−4] scientific interest has been recently rekindled by the desire to use it to enhance the efficiency of photovoltaic devices.[5] This is because each triplet exciton can, in principle, be dissociated into its component electron and hole, thereby enhancing the photocurrent.[6−9] Accordingly, increased power conversion efficiency is possible if a low-bandgap solar cell is sensitized with a high-bandgap material which undergoes fission[10−12]

Crystalline tetracene, the member of the acene family with four conjugated benzene rings, was the chief material used in historical studies of singlet fission.[1] This was because the comparable energies of the lowest-lying singlet and the triplet pair allow fission to proceed, but also permit the observation of delayed fluorescence from singlet excitons regenerated through triplet−triplet annihilation.[1,13,14] This is in contrast to highly luminescent three-ringed anthracene, where singlet fission is energetically unfavorable (i.e., the triplet exciton has significantly more than half of the energy of the lowest-lying singlet[1,2,15]), as well as nonemissive pentacene, where the energy levels are such that fission proceeds readily and unidirectionally.[16−20]

The key experimental result confirming the presence of exciton fission in tetracene was the demonstration that the magnitude of the "prompt" fluorescence was dependent on the strength and orientation of an external magnetic field.[3,13] Theories were developed that successfully described this behavior by taking into account the coupling between the emissive singlet and the fission-generated spin-correlated triplet pair, as well as the subsequent diffusional motion of triplets.[4,21−23] These theories have also been used to explain observations of field-dependent photocurrent modulation,[10] as well as time-dependent "quantum beating" in the photoluminescence (PL) intensity,[24−26] which was postulated to arise due to the time evolution of the nonstationary singlet-coupled triplet pair. All of these results offer clear evidence that singlet fission does proceed in tetracene at room temperature.

However, it was also observed that the magnitude of these effects varied as the sample was cooled, and that they often appeared to vanish at cryogenic temperatures.[3,10,13,26,27] This, combined with indirect measurements of the singlet and triplet energies suggesting that fission was endothermic (∼180 meV[1,14]), led to the acceptance of a thermally activated model for the fission process.[1,16,17] However, the recent demonstration by both Burdett et al. and Tayebjee et al. that the rate of the prompt (<100 ps) PL decay from tetracene shows no appreciable temperature dependence have cast doubt on the long-held thermally activated model,[28,29] though the underlying mechanisms proposed by the two groups differ.

Though the numerous time-resolved fluorescence studies of tetracene have provided information on the population dynamics of emissive singlet excitons,[29−32] there have been comparatively few reported experiments which directly probe

Received: August 27, 2013
Published: October 22, 2013

   dx.doi.org/10.1021/ja408854u | J. Am. Chem. Soc. 2013, 135, 16680−16688

the dynamics of nonemissive species, which has hampered the establishment of a consensus interpretation. An early study using single-wavelength transient absorption (TA) spectroscopy by Frolov et al.[33] identified two broad photoinduced absorption (PIA) features. They peaked at 780 nm (670 nm), and exhibited growth (decay) dynamics comparable to the stimulated emission (SE). However, the authors argued that singlet fission was not efficient in their vapor-grown crystals, ruled out the presence of triplets due to disagreement with the PIA spectrum of the triplet in solution, and instead assigned the features to radiative (trapped, nonemissive) singlet excitons.[33] By contrast, Thørsmolle et al. interpreted the results of their similar TA measurements on tetracene single crystals as evidence that a large triplet population was generated through two channels, one sub-picosecond channel that gave rise to 50% of the signal, and a second, thermally activated channel occurring on a 50 ps time scale that was responsible for the remainder.[17] Lastly, Grumstrup et al. associated the rapid rise of a PIA feature at 500 nm with the generation of triplet excitons, and explored the effect of temporally shaping the excitation pulse.[34]

More recently, a pair of papers from Burdett et al. offered a contrasting interpretation. Measuring tetracene in solution, they noted that the singlet exciton was associated with a trio of PIA features at 450, 650, and 1200 nm,[35] which decayed with a time constant (~4.2 ns) that was comparable to the separately measured fluorescence lifetime, as well as literature results.[36,37] At long times (~20 ns) after excitation, when the only remaining population is assumed to be triplet excitons resulting from intersystem crossing, they observed a PIA feature centered at ~470 nm[35] that was consistent with previous flash-photolysis results.[1] Measuring evaporated films of tetracene, the authors demonstrated that the mutually consistent singlet dynamics (~100 ps) could be measured with time-resolved PL and via the SE in TA, but only when using an initial excitation density of $\sim 2 \times 10^{17}$ cm^3 to suppress bimolecular recombination.[28] However, the authors noted that the triplet PIA at ~470 nm in the film was very weak relative to the strong transition observed in solution.[35] This, combined with the highly congested TA spectrum <530 nm and the limited signal-to-noise, meant that the population dynamics of triplets were not observed.[28] Additionally, we note that the experimental apparatus used did not allow the probing of the wavelength range around 800 nm to observe the PIA feature centered at ~780 nm that had been observed in single crystals,[17,33] but is absent in solution.[1,35] Hence, to address the controversy regarding the nature of photoexcited states by directly observing fission-generated triplets, and thereby explore the underlying mechanism of singlet exciton fission, we performed high-sensitivity, broad-band, ultrafast transient absorption on polycrystalline tetracene.

EXPERIMENTAL SECTION

We fabricated 70 nm films on silica substrates using thermal evaporation of tetracene powder (Sigma-Aldrich, #698415). Raw materials and samples were held under a nitrogen atmosphere until measurement, which was performed following encapsulation with a glass coverslip and cyanoacrylate glue for room-temperature measurements, or the helium atmosphere of a continuous-flow cryostat (Oxford Instruments Optistat). Temperature-dependent absorption spectra were measured with an Agilent Cary 6000i UV−vis−near-IR dual-beam spectrophotometer. For these measurements, we allowed the sample temperature to equilibrate for 30 min before taking data, and accounted for changes to the substrate transmission by using the second optical path to measure a blank. Temperature-dependent PL measurements were made by exciting the sample with a 40 MHz train of laser pulses with a duration of ~100 ps and a center wavelength of 470 nm (PicoQuant, LDH470). The PL was collected and directed to a 500 mm focal length imaging spectrograph (Princeton Instruments, SpectraPro2500i) fitted with a cooled CCD camera (PI Acton, PIXIS 100F).

For sub-picosecond TA spectroscopy, samples were excited with tunable, narrowband (~10 nm) ultrafast pulses derived from the output of a 1 kHz regenerative amplifier (Spectra-Physics Solstice) using a home-built non-collinear optical parametric amplifier (NOPA) modeled after Cerullo et al.[38] For nanosecond TA measurements, the frequency-doubled output (532 nm) of a Q-switched Nd:YVO_4 laser (Advanced Optical Technologies AOT-YVO-25QSPX) was employed as the pump to allow for the use of electronic delay. The transmission of the sample was probed using either the laser fundamental (770−830 nm), or the broadband (~520−790 nm) output of a second home-built NOPA. The probe beam was split to provide a reference signal not affected by the pump to mitigate the effect of laser fluctuations. The probe and reference signals were dispersed in a spectrometer (Andor, Shamrock SR-303i) and detected using a pair of 16-bit, 1024-pixel linear image sensors (Hamamatsu, S8381-1024Q), which were driven and read out at 1 kHz by a custom-built board from Stresing Entwicklunsbüro.

During measurement, alternate pump pulses were blocked using an optical chopper, so that the normalized differential transmission spectrum ($\Delta T/T$) could be calculated. Effects such as ground-state bleaching (GSB), photoinduced absorption (PIA), stimulated emission (SE), and thermal modulation can all contribute to the TA signal, as has has been described in detail elsewhere.[6,18−20] Generally 1000 "pump on" and "pump off" shots were averaged for each time point, and the entire range was measured 2−50 times. In sum, our apparatus allowed the detection of $\Delta T/T$ signals as small as 10^{-5} (broad-band probe), or 10^{-6} (800 nm probe). This enabled us to perform ultrafast, broad-band TA experiments at a sufficiently low excitation density ($\sim 2 \times 10^{17}$ cm^3) to minimize bimolecular recombination of the singlet at early times.[28] As we will demonstrate, these capabilities were critically necessary to obtain an accurate measure of the intrinsic dynamics.

Lastly, we note that the total average power of the pump and probe beams was ~30 μW, which was 100 times less than the intensity used in measuring the PL spectrum (see Figure 2 below). Given the close correspondence between our PL spectra and literature results, we do not expect that the sample experienced significant steady-state heating due to the laser pulse during TA. By contrast, as we have described previously[19,39] some transient, local heating is expected to occur in TA. If we make the assumption that all of the absorbed pump photons dissipate their heat instantaneously and consider a heat capacity similar to PMMA at 10 K,[40] this would generate heating within the pump spot on the order of 2 K, which would dissipate to the substrate before the next pulse.[39] A temperature increase of this scale is additionally consistent with the magnitude of the measured artifact from thermal modulation as discussed below.

RESULTS AND DISCUSSION

As the shape of the linear absorption spectrum is critical for the interpretation of the TA data, we present the evolution of the ground-state absorption spectrum as a function of temperature in Figure 1. We consider the features in the spectrum at room temperature to represent the Davydov-split absorption of the lowest-lying singlet exciton (506 and 524 nm) along with vibrational sidebands (483 and 474 nm as well as 456 and 444 nm).[1,4142] As the sample is cooled, we observe an apparent redistribution of the oscillator strength to the lower-energy Davydov peak in each of the two lowest-energy pairs, and note the large number of isosbestic points on the spectra. These are consistent with a spectrum that is the linear combination of contributions from two absorptive species that undergo temperature-dependent interconversion. This could result from the reported, incomplete temperature-dependent phase

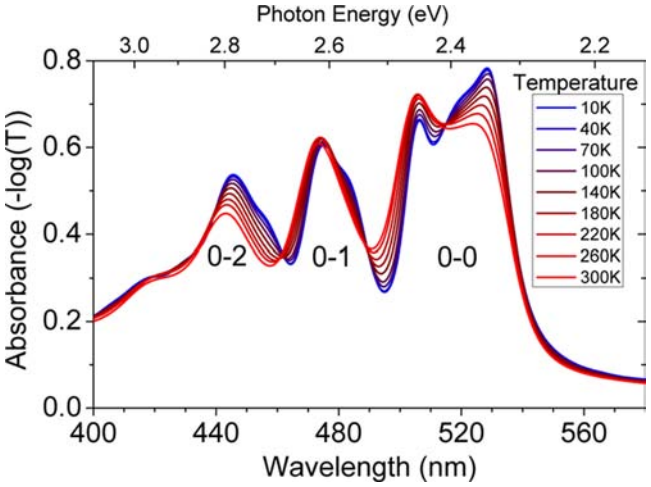

Figure 1. Ground-state absorption spectrum of an 80-nm-thick evaporated film of tetracene measured as a function of temperature. The Davydov-split peaks previously attributed[41] to vibrational sidebands are labeled. A substantial fraction of the apparent residual absorption at wavelengths longer than 560 nm is due to reflection from the interfaces.

transition in single crystals, and the existence of at least two polymorphs in vacuum-grown polycrystalline films,[43,44] perhaps complicated by the established effects of birefringence and anisotropic absorption.[45−47] Lastly, in anticipation of the need to account for the effect of temperature modulation by the pump pulse on the TA spectrum as established elsewhere,[19,39] we include a curve ("thermal effect") that is proportional to the difference between the absorption spectra at 280 and 300 K in Figure 3b (below).

The steady-state PL spectrum is presented as a function of temperature in Figure 2. These results are consistent with previous reports and the reader is directed to recent comprehensive studies for time-resolved (~20 ps) data,[28,31,32] even though the role of singlet fission is only explicitly considered in ref 28. The emission shows a prominent 0−0

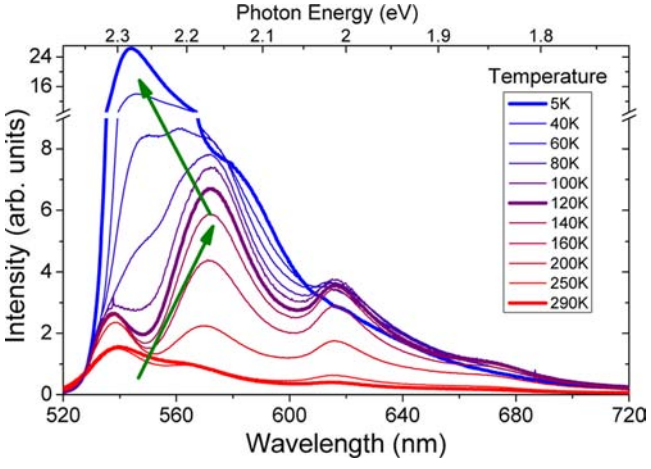

Figure 2. Temperature dependence of the PL spectrum of an 80 nm-thick tetracene film. Three curves are highlighted in the main graph to show the characteristic behavior at room (293 K), intermediate (120 K), and liquid helium (5 K) temperatures. We draw attention to the strength of the overall fluorescence enhancement, as well as the super-radiant enhancement of the ration of the 0−0:0−1 peaks at low temperatures, which necessitates the use of a vertical scale-break.

transition centered at ~537 nm at room temperature[48] along with additional transitions which have been assigned to vibrational sidebands and emission from defect sites.[31]

Upon cooling to 120 K, the emission features sharpen, and we observe a substantial increase in the signal at 573 nm, which has been attributed to emission from self-trapped excitons[31] as well as defect sites[28] presumed to result from the incomplete transition to the low-temperature polymorph.[43] Time-resolved luminescence data reported elsewhere[28,29,31] indicates that the 0−0 transition dominates the early time emission but decays rapidly ($\tau \approx 80$ ps).[28] By contrast, the emission at ~573 nm is less intense but much longer lived (>3 ns), and so dominates the integrated intensity.

As shown in Figure 2, cooling the sample further to 5 K causes a further, very large increase in the total fluorescence yield as well as an enhancement of the ratio of the 0−0 to the 0−1 vibronic peaks.[49] This increase in the integrated PL yield has been understood in terms of the reduced probability of nonradiative monomolecular recombination, as well as the super-radiant enhancement of the transition via delocalization.[30−32,50,51] We observe only slight further enhancement of the transition at 573 nm at these lowered temperatures and additionally note that the 0−1 emission from the primary radiative transition is also expected to have a contribution at these wavelengths.[31]

Figure 3a presents the picosecond-scale TA spectra of polycrystalline tetracene. Although we observed that the general spectral shape changed little with pump intensity, in agreement with Burdett et al.,[28] the initial decay dynamics were dramatically accelerated at elevated pump fluences. Thus, we do not consider an intensity-dependent spectral shape to be a sufficiently sensitive indicator of monomolecular dynamics. We found that the decay dynamics of the singlet were intensity-independent and largely monoexponential at excitation densities of $\sim 7 \times 10^{17}/\mathrm{cm}^3$ or lower (mean separation between excitations of ~7 nm) and used such fluences for all subsequent experiments (Figure S1).

Considering the TA spectra, we observe that the most pronounced feature at short times (~2 ps) is a positive peak centered at ~536 nm. This feature is formed within the instrument response (~200 fs) and diminishes in strength by ~70% over the first few hundreds of picoseconds while undergoing an apparent blue-shift to ~532 nm. We observe the parallel evolution of a peak/shoulder at ~570 nm, which decays to zero on a similar time scale without exhibiting any apparent spectral shift. The center wavelengths of the two peaks are in excellent agreement with the 0−0 and 0−1 peaks of the room-temperature PL spectrum (Figure 2). Hence, we assign the large positive contribution in the first 100 ps following excitation to SE. This is in agreement with literature results on thin films[28,35] and corresponds to the spectral position of a feature observed in single crystals, though we note that the SE in films appears to be relatively enhanced.[17,33] However, the observations contrast with the behavior of tetracene in solution,[35] where the TA signal in this region is uniformly negative due to a strong, overlapping PIA. Examining the $\Delta T/T$ signal in this spectral range beyond 100 ps, we observe a close correspondence between the location of the residual is "blue-shifted" peak at ~532 nm and the location of the expected peaks at ~527 nm from the GSB (Figure 1) and ~532 nm from the "thermal effect" (Figure 3b). Accordingly, we consider that the signal in this region at these times results from a combination of both effects.

dx.doi.org/10.1021/ja408854u | J. Am. Chem. Soc. 2013, 135, 16680−16688

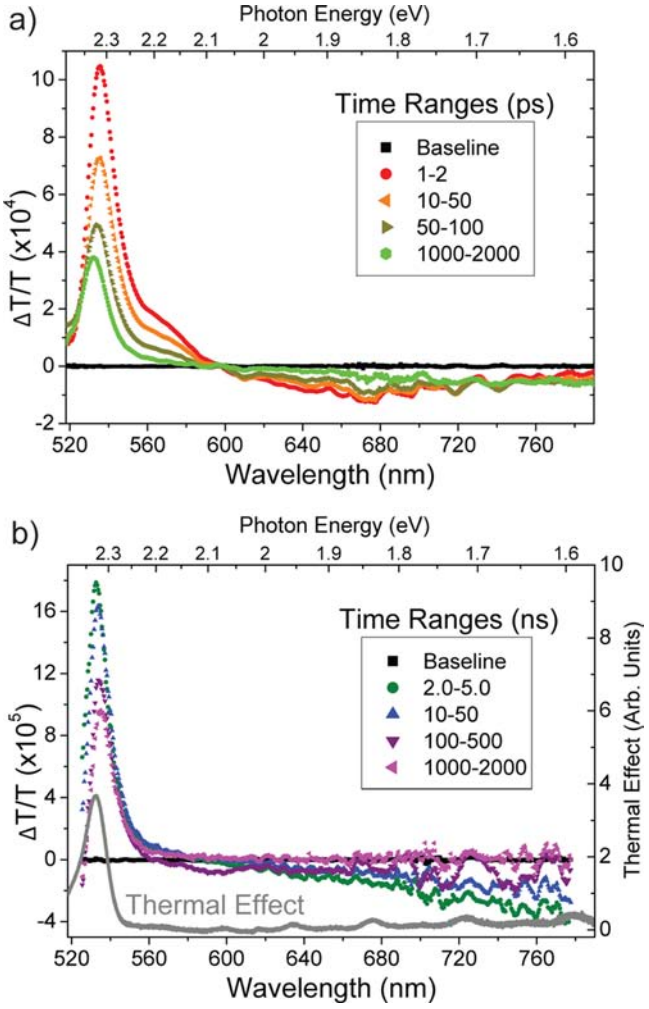

Figure 3. Time-dependent TA spectra of a tetracene film. Picosecond-scale data (a) were measured following excitation using ~100-fs-long pulses centered at 500 nm with an irradiance of ~8 μJ/cm^2 for an excitation density of ~5 × 10^{17}/cm^3. Nanosecond-scale data (b) were measured following excitation with ~600-ps-long pulses at 532 nm with an irradiance of ~4 μJ/cm^2 for an excitation density of ~6 × 10^{17}/cm^3. An additional curve is added to (b) that is proportional to the wavelength-dependent difference between the absorption of tetracene at 280 and 300 K, which is the expected shape of the "thermal effect". These data are plotted on the right-hand scale, where zero is vertically offset for clarity.

Looking at the TA signal in the remainder of the experimentally observed spectrum (600–800 nm), we observe two, broad PIA features with complementary dynamics and an isosbestic point at ~740 nm. The first PIA feature is centered at ~670 nm and rises within the experimental instrument response (~200 fs) before decaying in a similar manner to the SE. Unlike a previous report,[33] we observe no discrepancy between the rise of the SE and the rise of this feature. By contrast, the spectral shape and relative intensity of the PIA feature at ~670 nm are in good agreement with TA measurements on tetracene films made by Burdett et al.[28,35]

Before proposing an assignment for the PIA at 670 nm, we consider the second PIA feature that is responsible for the growth of the negative signal at wavelengths longer than 740 nm in Figure 3a. Examining the nanosecond-scale TA signal shown in Figure 3 b), we observe that this feature extends from ~600 nm to at least the end of the measurement range at 780 nm and is not observed to peak over this interval. It is also evidently the terminal excited state, as it decays without spectral evolution over tens of nanoseconds. These observations concur with the prominent and long-lived negative $\Delta T/T$ signal observed in the single-crystal TA measurements from Frolov et al.[33] and Thørsmolle et al.[17] that was assigned to PIA from trapped singlets and triplet excitons, respectively. To these considerations, we add that the thermal effect is not expected to contribute to the measured $\Delta T/T$ signal at any point in this entire (550–900 nm) wavelength range (Figure 3b), although it is likely responsible for the residual positive TA signal at ~532 nm at 1 μs.

Recalling that triplets are well-established to be the end-product of decay in tetracene at room temperature,[1,22,26] we assign the long-wavelength PIA feature to the excited-state absorption of the triplet exciton. This proposal is further supported by the calculations of Pabst and Köhn, who predict that the $T_1 \rightarrow T_2$ transition in molecular tetracene should have a center wavelength near 790 nm.[52] We address the frequently stated critique[1,33,35] that such a transition is not observed in isolated tetracene molecules in solution by highlighting our observation of an analogous long-wavelength PIA feature from triplet excitons in pentacene.[6,18,19] These results are all consistent with the oscillator strength of this transition being significantly enhanced in the solid state relative to the isolated molecule, which could occur if the monomolecular wave functions, particularly of the higher-lying T_2 state, were appreciably perturbed by intermolecular coupling.

Returning to the PIA feature at 670 nm, and noting its instantaneous onset (<200 fs), correspondence with an identified transition in monomeric tetracene in solution,[35] and the link to the long-wavelength triplet PIA feature via the isosbestic point at 740 nm, we associate this feature with the photogenerated singlet exciton. Thus the complementary decay of the PIA at 670 nm and growth of the PIA at 800 nm reflects the conversion of singlet excitons into triplets. Further, as has been argued for other materials (e.g., refs 17, 18, and 53–55), this evolution must occur via singlet exciton fission, as the time scale is short compared to what would be expected for intersystem crossing in the absence of heavy atoms or lone pairs.[1,56]

With the primary spectral features assigned, we made TA measurements at 30 K intervals from room temperature down to ~10 K to directly investigate the role of thermal activation in singlet exciton fission in tetracene. We note that the achievable signal-to-noise ratio using the broadband NOPA probe was reduced at low temperatures, particularly in the range from 650–800 nm, due to the considerable scattering from the sample itself, as well as the many air-glass interfaces in the cryostat. To allow experimentation at sufficiently low excitation densities, we employed the SE signal at 570 nm as a measure of the singlet population, and used the laser fundamental at 800 nm to probe the overlapping singlet + triplet PIA. This allowed the acquisition of TA signals with peak strengths of ~1 × 10^{-4} and ~3 × 10^{-5}, respectively, which correspond to excitation densities of ~4 × 10^{17}/cm^3 and ~8 × 10^{17}/cm^3. We note that the spectral shape of the TA signal in the range from 500 to 800 nm changes little as the temperature of the sample is varied in the range from 270 down to 10 K, other than the expected sharpening of the emission features, as well as some variation in the residual (long-time) signal around 520 nm that we attribute to the reported dynamic red-shift of the PL,[28] as well as the modification of the shape of the thermal effect (Figure S2)

dx.doi.org/10.1021/ja408854u | J. Am. Chem. Soc. 2013, 135, 16680–16688

Figure 4a presents the temporal evolution of the SE as a function of temperature. As the peak signal varied by ∼30% as

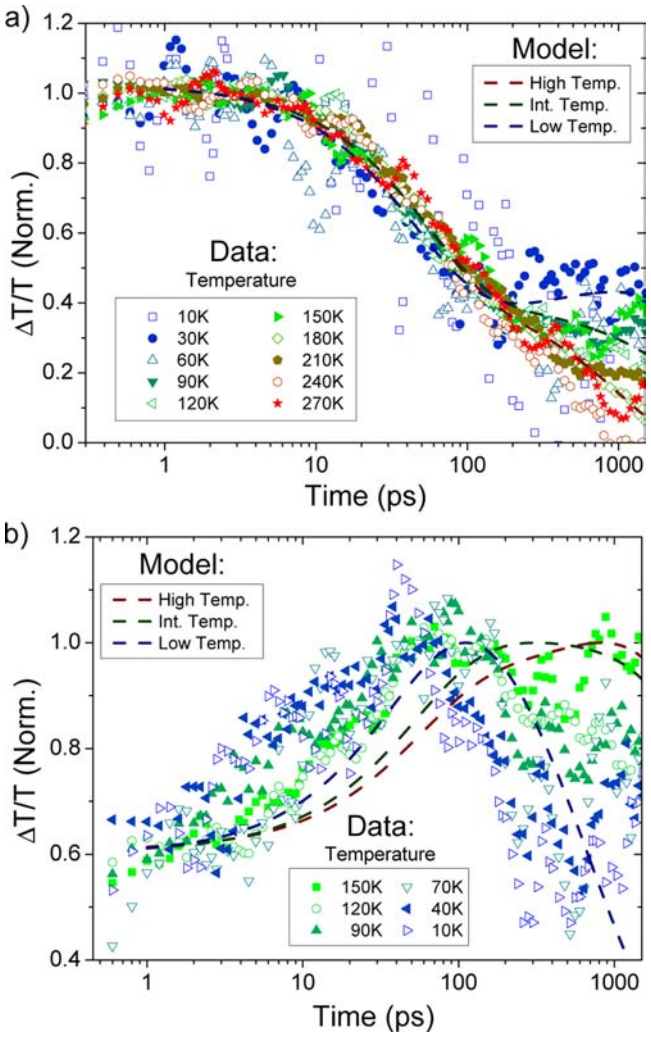

Figure 4. Temperature-dependent dynamics of the TA signal at (a) 560−580 nm and (b) 800 nm from a tetracene film excited with a 500 nm pump. At these time scales, the signal in (a) is substantially due to SE and thereby proportional to the population of singlet excitons, and the signal in (b) results from a linear combination of PIA features from the singlet and the triplet. The kinetic traces have been normalized by dividing by the mean value in the range (a) 0.5−5 ps or (b) 40−80 ps, which inverts the data in (b). Kinetic traces from the model described in eq 1 are added, and use consistent parameters between the plots, as listed in Table 1.

the sample was cooled, each kinetic trace has been normalized to the mean value from 0.5 to 5 ps. By inspection, it is evident that the decay dynamics of the SE in the first 200 ps exhibit no observable temperature dependence over the entire range of experimental temperatures (10−270 K). This result, with ∼200 fs time resolution and an excitation density of $\sim 4 \times 10^{17}/\mathrm{cm}^3$, is consistent with the earliest-resolvable fluorescence decay measured by Burdett et al.[28] using a streak camera with ∼20 ps time resolution. Subsequent to the primary decay process, we observe that the magnitude of the residual signal at 1 ns following excitation is greater at lower temperatures.

Figure 4b shows the corresponding temperature-dependent dynamics of the TA signal at 800 nm, normalized to the mean (negative) signal in the range 40−80 ps. Kinetic traces taken at temperatures greater than 150 K did not differ significantly over this time range, and so are omitted for clarity. We observe that the signal reaches ∼50% of its final value within the 200 fs instrument response, and subsequently grows to attain its maximum value over the next ∼100 ps. From the spectral assignments made previously, we consider that the signal is made up of PIA contributions from the instantaneously formed singlet, and the subsequently generated triplet pair. Thus, the dynamics we observe reflect the interconversion of singlet and triplet excitons, viz. singlet exciton fission, and, from the change in signal amplitude as singlets are converted to triplets, we find that the two species have oscillator strengths in a ratio of ∼1:2 at this wavelength. However, as is apparent, the dynamics show only slight dependence on temperature over the first 100 ps, which is inconsistent with the orders-of-magnitude difference in the rate that would be expected if fission were an conventional, Arrhenius-type, thermally activated process. We emphasize that the our measurements show that the dynamics of *both* the decay of the singlet and the growth of the triplet populations are largely unaffected by temperature in the range from 10−270 K. Hence, we consider that the rate of singlet fission itself is temperature-independent.

Subsequent to fission, the TA signal at 800 nm is largely static (100 ps−1 ns) when $T > 150$ K, but exhibits accelerated decay at cryogenic temperatures. Hence, we consider mechanisms which could lead to the loss of excited-state population on a sub-nanosecond time scale under these conditions. Recalling the significant increase in the steady-state PL when the sample is cooled (Figure 2), any hypothesis should additionally be consistent with increased time-integrated radiative emission from the singlet. Importantly, it has been shown that the radiative rate is accelerated from the room-temperature value (∼12.5 ns) by an order of magnitude at low temperatures due to super-radiance.[30,32] Consequently, if the expected slowing of the spatial diffusion of fission-generated triplet pairs at low temperatures allowed emissive singlets to be readily regenerated, the equilibrium population of singlets and triplet pairs might be "drained" by radiative decay of the singlet. However, this effect alone cannot be a complete explanation of our data, as the decoupling of the observed dynamics of emissive singlets (Figure 4 a) and triplets (Figure 4 b) is not compatible with the continued free interconversion between these states.

To illustrate this, we construct a toy model consisting of set of rate equations corresponding to a five-state system (ground, singlet ("free" and "trapped"), and triplet ("free" and "paired")) as shown schematically in Figure 5, and mathematically in the following:

$$\begin{aligned}
\dot{N}_{S(\mathrm{free})} &= -(k_{\mathrm{rad}} + k_{\mathrm{fis}} + k_{\mathrm{trap}})N_{S(\mathrm{free})} + (k_{\mathrm{fus}})N_{T(\mathrm{pair})} \\
\dot{N}_{S(\mathrm{trap})} &= -(k_{\mathrm{trapdec}})N_{S(\mathrm{trap})} + (k_{\mathrm{trap}})N_{S(\mathrm{free})} \\
\dot{N}_{T(\mathrm{pair})} &= -(k_{\mathrm{fus}} + k_{\mathrm{diss}} + k_{\mathrm{nrad}})N_{T(\mathrm{pair})} + (k_{\mathrm{fis}})N_{S(\mathrm{free})} \\
\dot{N}_{T(\mathrm{free})} &= -(k_{\mathrm{nrad}})N_{T(\mathrm{free})} + (2k_{\mathrm{diss}})N_{T(\mathrm{pair})}
\end{aligned} \tag{1}$$

where the N_x are the time-dependent populations of states x, and the $k_y = 1/\tau_y$ are first-order rate constants.

We assume that observed SE signal at 570 nm is proportional to the total number of singlets (free and trapped), and the PIA signal at 800 nm is given by a linear combination of the total singlet and triplet population, with a parameter, *OscR*, which

dx.doi.org/10.1021/ja408854u | J. Am. Chem. Soc. 2013, 135, 16680−16688

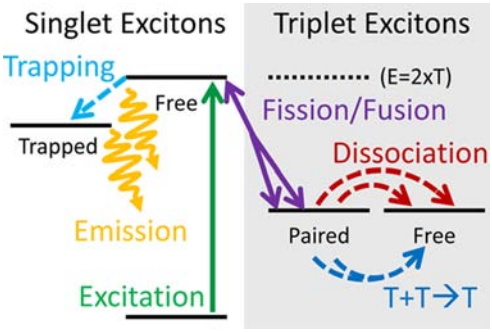

Figure 5. Schematic illustration of the photophysical model used to describe the photophysics observed in the three temperature ranges. We add a level at twice the energy of the isolated triplet to emphasize that fission from one singlet to a triplet pair is nearly isoenergetic. The geminate T+T→T process is only considered in the alternative kinetic scheme discussed below, and described algebraically in eq S1.

reflects the ∼1:2 ratio of their oscillator strengths at this wavelength and is used to match the experimental PIA signal at 2 ps. Algebraically,

$$\mathrm{PIA}(t) = OscR(N_{S(\mathrm{free})} + N_{S(\mathrm{trap})}) + (2N_{T(\mathrm{pair})} + N_{T(\mathrm{free})})$$

which is subsequently normalized to the peak value.

With photoexcitation assumed to yield a population that is 100% singlet excitons, a fission time ($S_1 \rightarrow 2T_1$) of 90 ps and fusion time ($2T_1 \rightarrow S_1$) of 160 ps largely capture both the early time decay dynamics and the onset time of the "kink" (peak) in the SE (PIA) for all temperatures (Figure 4). We note that this 90 ps time constant compares well with the early time kinetics of transient PL decay measured elsewhere,[28,29,34] and we suspect that part of the apparent acceleration of the PIA kinetics that we observe stems from bimolecular recombination at the slightly elevated (8 vs $4 \times 10^{17}/\mathrm{cm}^3$) excitation density, relative to the SE measurements, required to produce detectable PIA signal at all temperatures (Figure S3).

As the remaining parameters of the model are poorly constrained in general, we take an effective first-order decay time (20 ns) of the residual triplet population from the measured nanosecond-scale decay of the GSB (Figure S4), and consider three key illustrative cases. The specific parameters used to generate the curves in Figure 4 are summarized in Table 1. At high (room) temperature, where the radiative rate is slow (∼12.5 ns),[30,32] we observe that the SE continues to decay after 100 ps, while that PIA signal at 800 nm remains essentially unchanged. This is consistent with the spatial dissociation of triplet pairs, as this process is unlikely to affect the PIA from triplets, but would quench PL by slowing the effective rate of triplet fusion, thus shifting the singlet ⇌ triplet-pair equilibrium away from emissive singlets. Although a full treatment of the diffusional dynamics, in the manner of Suna,[21] is beyond the scope of this work, we are able to parametrize the measured data by adding a single channel for the dissociation of bound triplets with a characteristic time of 600 ps.

Table 1. Parameters Used To Generate the Modeled Curves in Figure 4

	temperature			
symbol	high	int.	low	process
τ_{fis}	←	90 ps	→	fission (S→2T)
τ_{fus}	←	150 ps	→	fusion (2T→S)
τ_{rad}	12.5 ns	6.25 ns	400 ps	decay of free singlets
τ_{diss}	600 ps	1.2 ns	∞	triplet pair dissociation
τ_{trap}	∞	2.4 ns	400 ps	singlet trapping
τ_{trapdec}	←	6.25 ns	→	trapped singlets decay
τ_{nrad}	←	20 ns	→	free triplet decay
OscR	0.53	0.48	0.35	relative osc. strengths

At intermediate (∼150 K) temperatures, we find that the PIA dynamics after 100 ps are similar to those at room temperature, while we observe additional SE. This behavior could result from a slowing of the triplet dissociation process, or, as suggested by the red-shifted steady-state PL in Figure 2, from a fraction of the singlet population directly[28] or diffusionally[31] occupying lower-energy emissive sites which are unable to undergo fission. As a result, we add a first-order decay channel to our model to reflect the trapping of "free" singlets, but find that that our data is well-fit by a range of triplet-pair dissociation/singlet trapping rates. Thus, while the modeled curve at "intermediate temperature" in Figure 4 corresponds to a triplet-pair dissociation time of 1.2 ns and a singlet trapping time of 2.4 ps, further constraint would require additional data. Lastly, we note that the effect of superradiance is only expected to accelerate the radiative rate by a factor of 2 at these temperatures,[32] which is consistent with the 2-fold increase in the strength of the 0−0 peak that we observe in the steady-state PL. (Figure 2)

However, most intriguing is the low-temperature (<40 K) case, where we observe a further, small enhancement of the post-100 ps SE, but a precipitous decline of the PIA signal to a level as little as half of its peak value. Given that the initial dynamics of both singlet and triplets continue to show little temperature dependence, we consider that the primary decay process remains singlet exciton fission. However, the divergent dynamics of these two signals insist that the equilibrium between these populations is broken after the first few hundred picoseconds. With the assumption that diffusion-driven triplet diffusion is frozen out at these temperatures, one possibility, suggested by a straightforward extension of our intermediate-temperature model, is that the decay of the PIA reflects the accelerated population loss due to super-radiant emission, while the residual SE signal results from the population of "trapped" singlet excitons which cannot undergo fission. As shown in Figure 4b, our model gives qualitative agreement to the data when both the radiative and trapping rates of the singlet are 400 ps. Within our simple model, this would imply that ∼40% of the photoexcited singlet excitons become trapped and that the effect of superradiance is ∼3× greater than has been proposed elsewhere.[30,32] However, it is clear that these parameters are sensitive to the relative oscillator strengths of the "free" and "trapped" singlet excitons at this wavelength, which our data does not effectively constrain. Comparable results are obtained if we consider that a similarly sized population of "trapped" singlets is directly photoexcited.

An alternative hypothesis, suggested by the curious saturation of the decay of the PIA at ∼50% of its peak value at the lowest temperatures, is that geminate $T_1 + T_1 \rightarrow T_n$ recombination becomes allowed under these conditions. As this process is nominally spin-forbidden between the two singlet-coupled triplets created during a fission event, this would require that spin-dephasing is significantly enhanced. As suggested by the cartoon in Figure 5 and eq S1, we model this process by adding a channel by which a triplet pair can evolve into a *single* free triplet. As shown in Figure S6, we achieve agreement with our

dx.doi.org/10.1021/ja408854u | J. Am. Chem. Soc. 2013, 135, 16680−16688

experimental data by taking the low-temperature radiative decay time ($\tau_{rad} \approx 1250$ ns) from the work of Lim et al.,[30] and using a characteristic time of 400 ps for both the singlet-trapping and $T_1 + T_1 \rightarrow T_n$ processes. The residual SE signal would again presumably result from "trapped" singlets with a decay rate unaffected by superradiance. Although this hypothesis is consistent with the surprisingly rapid disappearance of the "quantum beats" in the fluorescence decay dynamics of single-crystal tetracene as the temperature is lowered,[26] further, direct study of the spin-dephasing process of fission-generated triplet pairs is warranted.

Finally, as a check that the temperature-independent dynamics we observed were not facilitated by the excess energy of singlet exciton immediately after photoexcitation, we made further measurements of the TA signal at 800 nm at 10 K as a function of the excitation wavelength. As shown in Figure S7, we observe no significant difference in the dynamics of fission as the center wavelength of the ∼10 nm bandwidth pump beam is scanned from above (400 nm) to below (525 nm) the inferred energy of the triplet pair (500 nm).[14] These ultrafast measurements are in agreement with the 20-ps-scale PL dynamics reported by Burdett et al.,[28] and suggests that "hot" photoexcited singlet excitons relax to the vibrational ground state before undergoing fission, which would be expected given the relatively slow (tens of picoseconds) dynamics of singlet fission in tetracene, compared to the rapid, sub-picosecond dynamics expected for carrier thermalization.[57]

CONCLUSIONS

In this work, we have studied the photophysics in polycrystalline tetracene films in order to study the dynamical process of singlet exciton fission. By performing broad-band transient absorption at excitation fluences sufficiently low to minimize bimolecular effects, we were able to directly monitor the populations of both emissive (singlet) and nonemissive (triplet) states. From these data, we have arrived at a consistent set of spectral assignments and an accompanying photophysical model that demonstrate that photoexcited singlets undergo exciton fission with an ∼90 ps characteristic time to form triplet pairs at room temperature. Further, we confirm, with ultrafast time resolution, that the primary decay channel for singlet excitons is independent of temperature and observe, critically, that this decay is matched by the growth of a population of triplet excitons at all temperatures (10−270 K). Hence, contrary to previous experiments, the interpretation of which may have been complicated by indirect measurement techniques, we conclude that the intrinsic dynamics of singlet exciton fission in tetracene are independent of temperature.

However, we find that the photophysics in tetracene subsequent to the primary fission process (>200 ps) do show clear temperature dependence. At temperatures above 100 K, simple consideration of the ongoing process of singlet regeneration via triplet−triplet recombination under the influence of suppressed triplet diffusion[21] and shallow traps/directly photoexcited defects[28,31] are sufficient to model our data. As a result, we consider that these phenomena are the likely explanation of the historically observed temperature-dependent behavior of several indirect observables (e.g., refs 2, 3, 26, 30).

In contrast, at very low temperatures, we observe a sharp decline in the triplet population to ∼50% of its peak value in the timerange from 100 ps to 1 ns. We find that this puzzling observation could be consistent with the complete suppression of triplet diffusion and greater-than-expected superradiant enhancement. Alternatively, it could result from accelerated spin-dephasing between the fission-generated triplet pairs in the cryogenic system, a hypothesis which would also explain the comparable disappearance of the "quantum beats" in the time-resolved PL.[26] However, it is apparent even from our steady-state temperature-dependent absorption and PL data that further morphological characterization of tetracene at low temperatures is needed before the photophysics will be fully unravelled.

Taken together, our data imply that the pre-eminent initial decay channel for the photoexcited singlet is fission to form triplet pairs, though subsequent singlet regeneration via triplet−triplet fusion can result in an appreciable time-integrated PL quantum yield. This is particularly relevant at low temperatures, where an enhanced radiative decay rate and slowed triplet diffusion are expected. Notably, even though singlet fission in tetracene occurs with a ∼90 ps time constant, which is 3 orders of magnitude less rapid than in pentacene,[18] we consider that it is also highly efficient. This is both because this time scale of fission remains much more rapid than the fluorescence decay rate of the isolated molecule in solution,[35] and also because one would expect the rate of any kinetically competitive non-radiative decay process to be modulated by the large range of experimental temperatures, resulting in an experimentally detectable effect. Thus, we consider radiative decay and fission to be the only two significant monomolecular decay channels for the singlet exciton in pure tetracene at room temperature.

These findings have several consequences. First, to satisfy energy conservation, our interpretation requires either that participating singlet and triplet-pair states are much closer in energy than previously estimated, or that a hitherto-neglected physical phenomenon permits their continued interconversion at very low temperatures. Although it has been recently suggested that this energetic deficit could be satisfied by the interplay of strong electronic coupling and entropic considerations for temperatures above 170 K,[58] this interpretation is inconsistent with the results of our more complete range of experimentally accessible temperatures. Further, we emphasize that the primary photophysical dynamics that we observe occur on the time scale of tens of picoseconds, which is longer than the usual electronic dephasing times in such systems.

However, as we observe a relatively slow reaction rate which is not limited by the need for thermal activation, we propose that singlet fission in tetracene may proceed via a tunneling mechanism in the weak-coupling limit. Given that this coupling would be expected to depend on the molecular geometry, it is perhaps surprising that we do not observe the fission rate to change in response to the predicted phase transition to a low-temperature polymorph. However, we note that very recent studies suggest that the influence of molecular geometry on singlet fission may be highly local.[55,59]

More broadly, these results establish that the initial generation of triplet pairs from photoexcited singlet excitons can be efficient, even in materials where the process is relatively slow and the lack of a strong exothermic drive means that fission should be thought of as an equilibrium-like process between the singlet and triplet-pair populations. This has considerable technological significance, as higher-optical-gap materials such as tetracene could yield photovoltaic devices with larger open-circuit voltages and, most notably, may be able to be coupled to existing silicon-based solar cell technologies without intermediaries.[60] As a result, from the perspective of

employing singlet fission to better harness energy from the sun, this work indicates that the major hurdle to be overcome is not in triplet generation *per se*, but in the "exciton management" required to ensure efficient triplet dissociation and subsequent charge collection.

■ ASSOCIATED CONTENT

Supporting Information

Intensity-dependent TA kinetics, temperature-dependent TA spectra, parameters and curves for a kinetic model including a $T_1 + T_1 \rightarrow T_n$ channel, and excitation-wavelength-dependent TA kinetics. This material is available free of charge via the Internet at http://pubs.acs.org

■ AUTHOR INFORMATION

Corresponding Authors

mwbw@mit.edu
rhf10@cam.ac.uk

Present Addresses

[‡]Department of Chemistry, Massachusetts Institute of Technology, Cambridge MA 02139
[¶]Institut für Physik and Astronomie, Universität Potsdam, 14476 Potsdam-Golm, Germany

Notes

The authors declare no competing financial interest.

■ ACKNOWLEDGMENTS

We thank Chris Bardeen and John Burdett for helpful discussions, and acknowledge the support of the Engineering and Physical Sciences Research Council.

■ REFERENCES

(1) Smith, M. B.; Michl, J. *Chem. Rev.* **2010**, *110*, 6891−6936.
(2) Singh, S.; Jones, W. J.; Siebrand, W.; Stoicheff, B. P.; Schneider, W. G. *J. Chem. Phys.* **1965**, *42*, 330−342.
(3) Geacintov, N. E.; Pope, M.; Vogel, F. *Phys. Rev. Lett.* **1969**, *22*, 593−596.
(4) Merrifield, R. E.; Avakian, P.; Groff, R. P. *Chem. Phys. Lett.* **1969**, *3*, 386−388.
(5) Hanna, M. C.; Nozik, A. J. *J. Appl. Phys.* **2006**, *100*, 074510.
(6) Rao, A.; Wilson, M. W. B.; Hodgkiss, J. M.; Albert-Seifried, S.; Bässler, H.; Friend, R. H. *J. Am. Chem. Soc.* **2010**, *132*, 12698−12703.
(7) Lee, J.; Jadhav, P. J.; Baldo, M. A. *Appl. Phys. Lett.* **2009**, *95*, 033301.
(8) Reusswig, P. D.; Congreve, D. N.; Thompson, N. J.; Baldo, M. A. *Appl. Phys. Lett.* **2012**, *101*, 113304.
(9) Congreve, D. N.; Lee, J.; Thompson, N. J.; Hontz, E.; Yost, S. R.; Reusswig, P. D.; Bahlke, M. E.; Reineke, S.; Van Voorhis, T.; Baldo, M. A. *Science* **2013**, *340*, 334−337.
(10) Jadhav, P. J.; Mohanty, A.; Sussman, J. M.; Lee, J.; Baldo, M. A. *Nano Lett.* **2011**, *11*, 1495−1498.
(11) Ehrler, B.; Wilson, M. W. B.; Rao, A.; Friend, R. H.; Greenham, N. C. *Nano Lett.* **2012**, *12*, 1053−1057.
(12) Ehrler, B.; Walker, B. J.; Böhm, M. L.; Wilson, M. W. B.; Vaynzof, Y.; Friend, R. H.; Greenham, N. C. *Nat. Commun.* **2012**, *3*, 1019.
(13) Groff, R. P.; Avakian, P.; Merrifield, R. E. *Phys. Rev. B* **1970**, *1*, 815−817.
(14) Tomkiewicz, Y.; Groff, R. P.; Avakian, P. *J. Chem. Phys.* **1971**, *54*, 4504.
(15) Klein, G.; Voltz, R.; Schott, M. *Chem. Phys. Lett.* **1973**, *19*, 391−394.
(16) Jundt, C.; Klein, G.; Sipp, B.; Le Moigne, J.; Joucla, M.; Villaeys, A. A. *Chem. Phys. Lett.* **1995**, *241*, 84−88.
(17) Thorsmølle, V. K.; Averitt, R. D.; Demsar, J.; Smith, D. L.; Tretiak, S.; Martin, R. L.; Chi, X.; Crone, B. K.; Ramirez, A. P.; Taylor, A. J. *Phys. Rev. Lett.* **2009**, *102*, 017401.
(18) Wilson, M. W. B.; Rao, A.; Clark, J.; Kumar, R. S. S.; Brida, D.; Cerullo, G.; Friend, R. H. *J. Am. Chem. Soc.* **2011**, *133*, 11830−11833.
(19) Rao, A.; Wilson, M. W. B.; Albert-Seifried, S.; Di Pietro, R.; Friend, R. H. *Phys. Rev. B* **2011**, *84*, 195411.
(20) Wilson, M. W. B.; Rao, A.; Ehrler, B.; Friend, R. H. *Acc. Chem. Res.* **2013**, *46*, 1330−1338.
(21) Suna, A. *Phys. Rev. B* **1970**, *1*, 1716−1739.
(22) Bouchriha, H.; Ern, V.; Fave, J. L.; Guthmann, C.; Schott, M. *Phys. Rev. B* **1978**, *18*, 525−528.
(23) Klein, G. *Chem. Phys. Lett.* **1978**, *57*, 202−206.
(24) Chabr, M.; Wild, U. P.; Fünfschilling, J.; Zschokke-Gränacher, I. *Chem. Phys.* **1981**, *57*, 425−430.
(25) Fünfschilling, J.; Zschokke-Gränacher, I.; Canonica, S.; Wild, U. P. *Helv. Phys. Acta* **1985**, *58*, 347−354.
(26) Burdett, J. J.; Bardeen, C. J. *J. Am. Chem. Soc.* **2012**, *134*, 8597−8607.
(27) Merrifield, R. E. *Pure Appl. Chem.* **1971**, *27*, 481−498.
(28) Burdett, J. J.; Gosztola, D.; Bardeen, C. J. *J. Chem. Phys.* **2011**, *135*, 214508.
(29) Tayebjee, M. J. Y.; Clady, R. G. C. R.; Schmidt, T. W. *Phys. Chem. Chem. Phys.* **2013**, *15*, 14797−14805.
(30) Lim, S.-H.; Bjorklund, T. G.; Spano, F. C.; Bardeen, C. J. *Phys. Rev. Lett.* **2004**, *92*, 10−13.
(31) Voigt, M.; Langner, A.; Schouwink, P.; Lupton, J. M.; Mahrt, R. F.; Sokolowski, M. *J. Chem. Phys.* **2007**, *127*, 114705.
(32) Camposeo, A.; Polo, M.; Tavazzi, S.; Silvestri, L.; Spearman, P.; Cingolani, R.; Pisignano, D. *Phys. Rev. B* **2010**, *81*, 1−4.
(33) Frolov, S. V.; Kloc, C.; Schön, J. H.; Batlogg, B. *Chem. Phys. Lett.* **2001**, *334*, 65−68.
(34) Grumstrup, E.; Johnson, J. C.; Damrauer, N. *Phys. Rev. Lett.* **2010**, *105*, 1−4.
(35) Burdett, J. J.; Müller, A. M.; Gosztola, D.; Bardeen, C. J. *J. Chem. Phys.* **2010**, *133*, 144506.
(36) Burgdorff, C.; Ehrhardt, S.; Löhmannsröben, H. G. *J. Phys. Chem.* **1991**, *95*, 4246−4249.
(37) Okajima, S.; Lim, E. C. *Chem. Phys. Lett.* **1976**, *37*, 403−407.
(38) Manzoni, C.; Polli, D.; Cerullo, G. *Rev. Sci. Instrum.* **2006**, *77*, 023103.
(39) Albert-Seifried, S.; Friend, R. H. *Appl. Phys. Lett.* **2011**, *98*, 223304.
(40) Zeller, R. C.; Pohl, R. O. *Phys. Rev. B* **1971**, *4*, 2029−2041.
(41) Yamagata, H.; Norton, J. E.; Hontz, E.; Olivier, Y.; Beljonne, D.; Brédas, J.-L.; Silbey, R. J.; Spano, F. C. *J. Chem. Phys.* **2011**, *134*, 204703.
(42) Following convention, we label the transition between the *m*th vibrational sublevel of the electronic ground state and the *n*th sublevel of the electronic excited state as *m*−*n*.
(43) Venuti, E.; Della Valle, R. G.; Farina, L.; Brillante, A.; Masino, M.; Girlando, A. *Phys. Rev. B* **2004**, *70*, 1−8.
(44) Sondermann, U.; Kutoglu, A.; Bässler, H. *J. Phys. Chem.* **1985**, *89*, 1735−1741.
(45) Hofberger, W. *Phys. Stat. Sol. (a)* **1975**, *30*, 271−278.
(46) Hofberger, W. *Phys. Stat. Sol. (a)* **1976**, *34*, K55−K58.
(47) Irkhin, P.; Ryasnyanskiy, A.; Koehler, M.; Biaggio, I. *Phys. Rev. B* **2012**, *86*, 085143.
(48) We expect that apparent peak location of this transition is likely red-shifted due to the effect of self-absorption,[32] but note that this effect would apply equally to the SE signal in TA.
(49) The slight red-shifting of the center wavelength has been associated with the aforementioned structural transition at low temperatures.[31]
(50) Spano, F. C. *Annu. Rev. Phys. Chem.* **2006**, *57*, 217−243.
(51) Spano, F. C. *Acc. Chem. Res.* **2010**, *43*, 429−439.
(52) Pabst, M.; Köhn, A. *J. Chem. Phys.* **2008**, *129*, 214101.
(53) Johnson, J. C.; Nozik, A. J.; Michl, J. *J. Am. Chem. Soc.* **2010**, *132*, 16302−3.

(54) Ramanan, C.; Smeigh, A. L.; Anthony, J. E.; Marks, T. J.; Wasielewski, M. R. *J. Am. Chem. Soc.* **2012**, *134*, 386−397.
(55) Roberts, S. T.; McAnally, R. E.; Mastron, J. N.; Webber, D. H.; Whited, M. T.; Brutchey, R. L.; Thompson, M. E.; Bradforth, S. E. *J. Am. Chem. Soc.* **2012**, *134*, 6388−6400.
(56) Köhler, A.; Bässler, H. *Mater. Sci. Eng. R* **2009**, *66*, 71−109.
(57) Bakulin, A. A.; Rao, A.; Pavelyev, V. G.; van Loosdrecht, P. H. M.; Pshenichnikov, M. S.; Niedzialek, D.; Cornil, J.; Beljonne, D.; Friend, R. H. *Science* **2012**, *335*, 1340−1344.
(58) Chan, W.-L.; Ligges, M.; Zhu, X.-Y. *Nat. Chem.* **2012**, *4*, 840−845.
(59) Piland, G. B.; Burdett, J. J.; Kurunthu, D.; Bardeen, C. J. *J. Phys. Chem. C* **2013**, *117*, 1224−1236.
(60) Ehrler, B.; Musselman, K. P.; Böhm, M. L.; Friend, R. H.; Greenham, N. C. *Appl. Phys. Lett.* **2012**, *101*, 153507.